



HAL
open science

cis-Cinnamic acid is a natural plant growth-promoting compound

Ward Steenackers, Ilias El Houari, Alexandra Baekelandt, Klaas Witvrouw, Stijn Dhondt, Olivier Leroux, Nathalie Gonzalez, Sander Corneillie, Igor Cesarino, Dirk Inzé, et al.

► To cite this version:

Ward Steenackers, Ilias El Houari, Alexandra Baekelandt, Klaas Witvrouw, Stijn Dhondt, et al.. cis-Cinnamic acid is a natural plant growth-promoting compound. *Journal of Experimental Botany*, 2019, 70 (21), pp.6293-6304. 10.1093/jxb/erz392 . hal-02624702

HAL Id: hal-02624702

<https://hal.inrae.fr/hal-02624702>

Submitted on 26 May 2020

HAL is a multi-disciplinary open access archive for the deposit and dissemination of scientific research documents, whether they are published or not. The documents may come from teaching and research institutions in France or abroad, or from public or private research centers.

L'archive ouverte pluridisciplinaire **HAL**, est destinée au dépôt et à la diffusion de documents scientifiques de niveau recherche, publiés ou non, émanant des établissements d'enseignement et de recherche français ou étrangers, des laboratoires publics ou privés.



Distributed under a Creative Commons Attribution - NonCommercial 4.0 International License



RESEARCH PAPER

cis-Cinnamic acid is a natural plant growth-promoting compound

Ward Steenackers^{1,2,*}, Ilias El Houari^{1,2,*}, Alexandra Baekelandt^{1,2}, Klaas Witvrouw^{1,2}, Stijn Dhondt^{1,2}, Olivier Leroux³, Nathalie Gonzalez^{1,2,†}, Sander Corneillie^{1,2,‡}, Igor Cesarino^{1,2,‡}, Dirk Inzé^{1,2,§}, Wout Boerjan^{1,2,§,¶} and Bartel Vanholme^{1,2,§,¶}

¹ Ghent University, Department of Plant Biotechnology and Bioinformatics, B-9052 Gent, Belgium

² VIB Center for Plant Systems Biology, VIB, Technologiepark 927, B-9052 Gent, Belgium

³ Ghent University, Department of Biology, B-9000 Gent, Belgium

[†] Present address: UMR 1332 Biologie du Fruit et Pathologie, INRA Bordeaux-Aquitaine Bât. IBVM71, av. Edouard Bourlaux, CS 20032, 33882 Villenave d'Ornon Cedex, France.

[‡] Present address: Department of Botany, Institute of Biosciences, University of São Paulo, Butantã, São Paulo, Brazil.

^{*} These authors contributed equally to this work and share first authorship.

[§] These authors share last authorship.

[¶] Correspondence: bartel.vanholme@psb.vib-ugent.be

Received 1 April 2019; Editorial decision 16 August 2019; Accepted 19 August 2019

Editor: Angus Murphy, University of Maryland, USA

Abstract

Agrochemicals provide vast potential to improve plant productivity, because they are easy to implement at low cost while not being restricted by species barriers as compared with breeding strategies. Despite the general interest, only a few compounds with growth-promoting activity have been described so far. Here, we add *cis*-cinnamic acid (*c*-CA) to the small portfolio of existing plant growth stimulators. When applied at low micromolar concentrations to *Arabidopsis* roots, *c*-CA stimulates both cell division and cell expansion in leaves. Our data support a model explaining the increase in shoot biomass as the consequence of a larger root system, which allows the plant to explore larger areas for resources. The requirement of the *cis*-configuration for the growth-promoting activity of CA was validated by implementing stable structural analogs of both *cis*- and *trans*-CA in this study. In a complementary approach, we used specific light conditions to prevent *cis/trans*-isomerization of CA during the experiment. In both cases, the *cis*-form stimulated plant growth, whereas the *trans*-form was inactive. Based on these data, we conclude that *c*-CA is an appealing lead compound representing a novel class of growth-promoting agrochemicals. Unraveling the underlying molecular mechanism could lead to the development of innovative strategies for boosting plant biomass.

Keywords: Agrochemical, auxin, biomass, biostimulant, *cis*-cinnamic acid, isomer, LED, phenylpropanoid, *trans*-cinnamic acid, UV, yield.

Introduction

Yield is the most important trait under study for crop improvement (Vanhaeren *et al.*, 2016) and one of the first that was effectively optimized thanks to consistent selection and

cultivation of the most productive plants over many generations (Hufford *et al.*, 2012; Hake and Ross-Ibarra, 2015). The integration of modern genetics with general plant breeding

techniques accelerated the increase in crop productivity even more (Evenson and Gollin, 2003). Although time consuming and labor intensive, this man-guided evolution of crops turned out to be an extremely efficient strategy, as illustrated by the 10-fold increase in the kernel weight of maize since its domestication (Liu *et al.*, 2016), and the 6-fold increase in corn production in the USA between 1940 and 2017 (from 1.8 t ha⁻¹ to 11.1 t ha⁻¹) after introduction of hybrid breeding strategies (Chavas and Mitchell, 2018).

Besides classical breeding, which exploits the natural variation in the gene pool, agrochemicals can be used as an alternative strategy to maximize plant yield. Compounds can be supplied on the spot without a restriction by species barriers, which is an important advantage compared with the breeding strategy and explains the general interest of companies in finding such molecules. Many of the currently commercially available growth-stimulating products are in fact (processed) extracts of an organic source (e.g. Kelp extract, humic substances, or protein hydrolysates), of which the bioactive substance or mode of action are often not known (Yakhin *et al.*, 2016). In addition, these heterogeneous mixtures suffer from batch-to-batch variation, creating a serious drawback to their applicability in the field. In this regard, a pure and well-characterized yield-promoting compound (YPC) allows a better standardization in its application, which should translate into a more consistent growth-stimulating effect on plants.

The discovery of plant hormones, which tightly regulate different aspects of plant development in low concentrations, came with high expectations to deploy these molecules as YPCs (Cholodny, 1936; Thimann and Lane, 1938; Willard, 1938). Unfortunately, over the following decades, it was clear that these compounds could not meet expectations (Leopold, 1955). A large number of different experiments demonstrated that the growth-promoting activity of phytohormones was extremely variable, setting the stage for the overall confusion about their applicability as YPCs (Kruyt, 1954). Moreover, the interpretation of the results was complicated by the characteristic pleiotropic effects of phytohormones, which are a mere consequence of the multiple intertwined pathways they steer combined with their typical tissue-dependent activity (Depuydt and Hardtke, 2011). In addition, hormones are physiologically active at very low concentrations within a narrow and species-dependent concentration range. These pitfalls are not limited to phytohormones, but also hold true for many bioactive compounds (Hardeland, 2016), which is reflected in the limited number of YPCs currently known (Arnao and Hernandez-Ruiz, 2019; Van Dingenen *et al.*, 2017).

One of the compounds with claimed growth-promoting activity is the phenylpropanoid cinnamic acid (CA) (Kick, 1953; Talaat and Balbaa, 2010; Singh *et al.*, 2013; Kurepa *et al.*, 2018). Like all phenylpropanoids, CA presents *cis/trans*-isomerism, and both isomers are endogenous to plants (Yin *et al.*, 2003; Wong *et al.*, 2005). The *trans*-isomer (*t*-CA) is the deamination product of the aromatic amino acid L-phenylalanine and is channeled into the phenylpropanoid pathway to produce a wide range of important secondary metabolites, including salicylic acid, flavonoids, and monolignols (Vanholme *et al.*, 2019). The *cis*-isomer (*c*-CA) is a photo-isomerization product of

t-CA. In contrast to its *trans*-isomer, *c*-CA is not channeled into the pathway, but has recently been identified as an inhibitor of polar auxin transport (Steenackers *et al.*, 2017). Accordingly, *c*-CA-treated Arabidopsis roots display a phenotype similar to that induced by high auxin concentrations, including primary root inhibition and lateral root proliferation (Wong *et al.*, 2005; Wasano *et al.*, 2013). Despite the mechanistic insights into the bioactivity of CA, its claimed growth-promoting activity is much less understood. Here, we show that *c*-CA and not *t*-CA is the bioactive form with growth-promoting activity. In addition, we demonstrate that auxin plays a crucial role in the CA-triggered biomass increase, but not directly at the level of the shoot. The results support a model explaining the increase in shoot biomass as a consequence of the *c*-CA-mediated proliferation of the root system.

Materials and methods

Plant material and growth conditions

Arabidopsis thaliana Col-0 seeds were surface-sterilized in 1.5 ml microcentrifuge tubes using vapor-phase seed sterilization. Briefly, the seed-containing tubes were placed overnight into a closed container along with a beaker containing 150 ml of NaOCl, to which 8 ml of HCl was added. The next day, the tubes were placed in a sterile laminar flow hood and left open for at least 3 h. Sterile Arabidopsis seeds were sown in square plates (12×12 cm) containing 0.8% (w/v) agar-solidified 0.5× Murashige and Skoog (MS) medium [1.5 g l⁻¹ MS basal salt mixture powder (Duchefa), 7.14 g l⁻¹ sucrose, 0.36 g l⁻¹ MES monohydrate, 8.0 g l⁻¹ plant tissue culture agar (Duchefa); pH 5.7]. After sowing, plates were incubated at 4 °C for 3 d for stratification, after which the plates were placed in a vertical or horizontal orientation in the tissue culture room under long-day growth conditions (16 h light/8 h dark) at 21 °C. The light spectra of the growth rooms were monitored with a PAR200 quantum spectrometer. The amount of UV-B was quantified with a SpectroSense2 meter equipped with a UV-B sensor (Sky Instruments).

Nicotiana benthamiana seeds were sterilized by soaking them in 70% ethanol for 2 min in a 2 ml microcentrifuge tube and subsequently for 10 min in a mixture of water and NaOCl (50/50) to which 0.05% Tween-20 was added. After sterilization, seeds were thoroughly rinsed with sterile distilled water and subsequently transferred to square plates (22.5×22.5 cm) or boxes (10.5×9.5×16 cm) containing 0.8% (w/v) agar-solidified 0.5× Gamborg B5 medium [1.5 g l⁻¹ Gamborg B5 basal salt mixture powder (Duchefa), 7.14 g l⁻¹ sucrose, 0.36 g l⁻¹ MES monohydrate, 8.0 g l⁻¹ plant tissue culture agar (Duchefa); pH 5.7]. After sowing, plates were incubated at 4 °C for at least 2 d and a maximum of 4 d, after which they were placed in a vertical or horizontal orientation in the tissue culture room under long-day growth conditions (16 h light/8 h dark) at 24 °C. A similar procedure was followed for boxes, with the exception that boxes were always placed in a horizontal orientation.

Compounds

All compounds were purchased from Sigma-Aldrich, except for *cis*-2-phenylcyclopropane-1-carboxylic acid (*c*-PCPCA), which was obtained from Mcule (P-4159565). Compounds were dissolved in DMSO at a concentration of 40 mM, and added at the desired concentration to the plant medium before pouring.

Root growth analysis

To quantify the effect of a given compound on root growth, seedlings were grown on vertically orientated square plates as described above. Thirteen days after stratification (DAS), plates were scanned using the Scanmaker 9800XL, and root length was measured using ImageJ software (Schneider

et al., 2012). The inhibitory concentration ($IC_{50-root}$) was calculated from the dose–response curve plotted in Sigma Plot. The numbers of adventitious roots (above the root–shoot junction) and of emerged lateral roots were counted using a stereomicroscope (CETI Binocular Zoom Stereo). The adventitious rooting assay was performed by incubating the plates in the dark for 7 d after a 4 h light treatment in the growth room to trigger germination. Plates were subsequently transferred to the growth chamber (16 h light/8 h dark) and incubated for another 7 d.

Projected rosette area and total leaf area of *A. thaliana* and *N. benthamiana*

The quantification of the projected rosette areas was performed on Arabidopsis plants grown on 0.5× MS medium in round Petri dishes (diameter 14.0 cm). The plates were positioned on a rotating platform, named IGIS, allowing fully automatic phenotyping over time (Dhondt *et al.*, 2014). Imaging was performed at a 6 min interval between consecutive plates (as a result, every plate on the platform was imaged once every hour), and near-IR technology was used to visualize plants in the dark. Projected rosette areas were automatically extracted from the images with C++ scripts using the OpenCV libraries, and a data analysis pipeline was used to compile the measurements and to construct rosette growth curves. For the leaf series, individual rosette leaves were removed from the plant at 20 or 23 DAS for *A. thaliana* or *N. benthamiana*, respectively. Leaves were oriented from old (cotyledons) to young on a thin layer of 1% (w/v) agar covering the bottom of a square plate (22.5×22.5 cm). The leaf series were subsequently imaged and the area of each individual leaf was determined using ImageJ (Schneider *et al.*, 2012).

Epidermal cell size measurements and image analysis

The third leaf of Arabidopsis (20 DAS) was harvested for cellular analysis. After clearing successively with 70% ethanol and 100% lactic acid, leaves were mounted in lactic acid on microscopic slides. The total leaf blade area was measured for 15 representative leaves per treatment under a dark-field stereomicroscope. Five leaves with an area closest to the median were used for detailed cellular analysis. Abaxial (lower) epidermal cells at the base of these leaves were drawn with a differential interference contrast microscope (Leica) equipped with a drawing tube. The microscopic drawings of the abaxial epidermis were scanned for digitalization. Processing of the microscopic images was done as previously described (Andriankaja *et al.*, 2012).

N. benthamiana stem sections

Stem segments of *N. benthamiana* were fixed in 4% (v/v) paraformaldehyde in PEM buffer (100 mM PIPES, 10 mM MgSO₄, 10 mM EGTA, pH 6.9) at room temperature for 2 h. After washing in demineralized water, stem segments were glued to the vibratome stage using superglue (Roticoll, Carl Roth). Sections of 60 μm thickness, prepared with a vibrating microtome (HM 650V, ThermoScientific, Germany), were stained with 0.5% (w/v) astra blue, 0.5% (w/v) chrysoidine, and 0.5% (w/v) acridine red, and mounted in Euparal (Roth) after dehydration in isopropyl alcohol. Slides were imaged with a Nikon Ni-U microscope equipped with a Nikon DS-Fi1c camera. Images were subsequently processed to quantify cell number, shape, and size, using the method described previously (Andriankaja *et al.*, 2012). Cellular analysis was performed on three regions from two independent sections obtained from three representative plants per treatment.

RNA extraction and quantitative real-time PCR (qRT-PCR) analysis

Roots and rosettes of mock-treated and 2.5 μM *c/t*-CA-treated Arabidopsis plants were harvested at 10 DAS from pools of 20 plants in 10 biological replicates. RNA extraction and cDNA synthesis were performed according to Baekelandt *et al.* (2018). The relative expression level of selected genes was determined with the Roche LightCycler 480 combined with the SYBR Green I Master Kit (Roche Diagnostics) in

three technical repeats using the primers listed in Supplementary Table S1 at JXB online. The qRT-PCR data were analyzed by normalizing the Ct values obtained for the genes of interest against those of two house-keeping genes (*CDKA1* and *EEF*).

GUS histochemical staining

β-Glucuronidase (GUS) assays were performed and inspected using differential interference contrast optics as described in Beeckman and Engler (1994).

Statistical analysis

Statistical analyses were performed using SAS Enterprise Guide 7 software. Either the Dunnett's test was implicated for ANOVA between the treatments and control group or an *F*-test was first used to assess equality of variances between treatment and control. Subsequently, the appropriate unpaired Student's *t*-test was performed to compare population means.

Results

The isomeric mixture *c/t*-CA promotes plant growth

To quantify the impact of CA on Arabidopsis rosette growth, a time-lapse analysis was performed using a fully automated phenotyping platform (Dhondt *et al.*, 2014). Arabidopsis seeds were germinated on 0.5× MS medium supplemented with different concentrations of CA (0, 1, 2.5, and 5 μM) and plant growth was followed over time by imaging the plants using a 1 h time interval. Images were subsequently processed via an automated image analysis pipeline to obtain information on the projected rosette area (see the Materials and methods for details). The CA concentrations were chosen based on the known $IC_{50-root}$ of CA (i.e. the CA concentration needed to reduce the primary root length by 50%), which is 9.2 μM under the conditions tested (Steenackers *et al.*, 2017). Although the *t*-CA was used to prepare the CA stock, we have previously shown that photo-isomerization of *t*-CA results in the accumulation of the bioactive *c*-CA during the growth period (Steenackers *et al.*, 2017). The isomeric mixture of CA will be further referred to as *c/t*-CA to distinguish it from the initially added *t*-CA (Fig. 1A). The end point of the experiment was set at 20 DAS and was determined by the onset of bolting.

Despite a clear trend towards increased rosette area of *c/t*-CA-treated plants over time, the difference was only significant at the end of the growth period (an increase of 17% and 24% upon treatment with 2.5 μM and 5 μM *c/t*-CA, respectively) (Fig. 1B; Supplementary Table S2). The difficulty in statistically supporting the growth-promoting effect of *c/t*-CA was mainly due to the focus on the projected rosette area as a proxy for the biomass. Although being the only realistic approach to follow plant growth over time, overlapping leaves result in an underestimation of the total leaf surface area (Dhondt *et al.*, 2014). To address this inadequacy, leaf series were made at the final time point (20 DAS), allowing the measurement of individual leaf areas as well as the correct area of a fully expanded rosette (Fig. 1C; Supplementary Table S3). The sum of individual leaf areas was significantly larger for *c/t*-CA-treated plants compared with that of controls (increase of 32, 32, and 28% for plants treated with 1, 2.5, and 5 μM *c/t*-CA, respectively). In

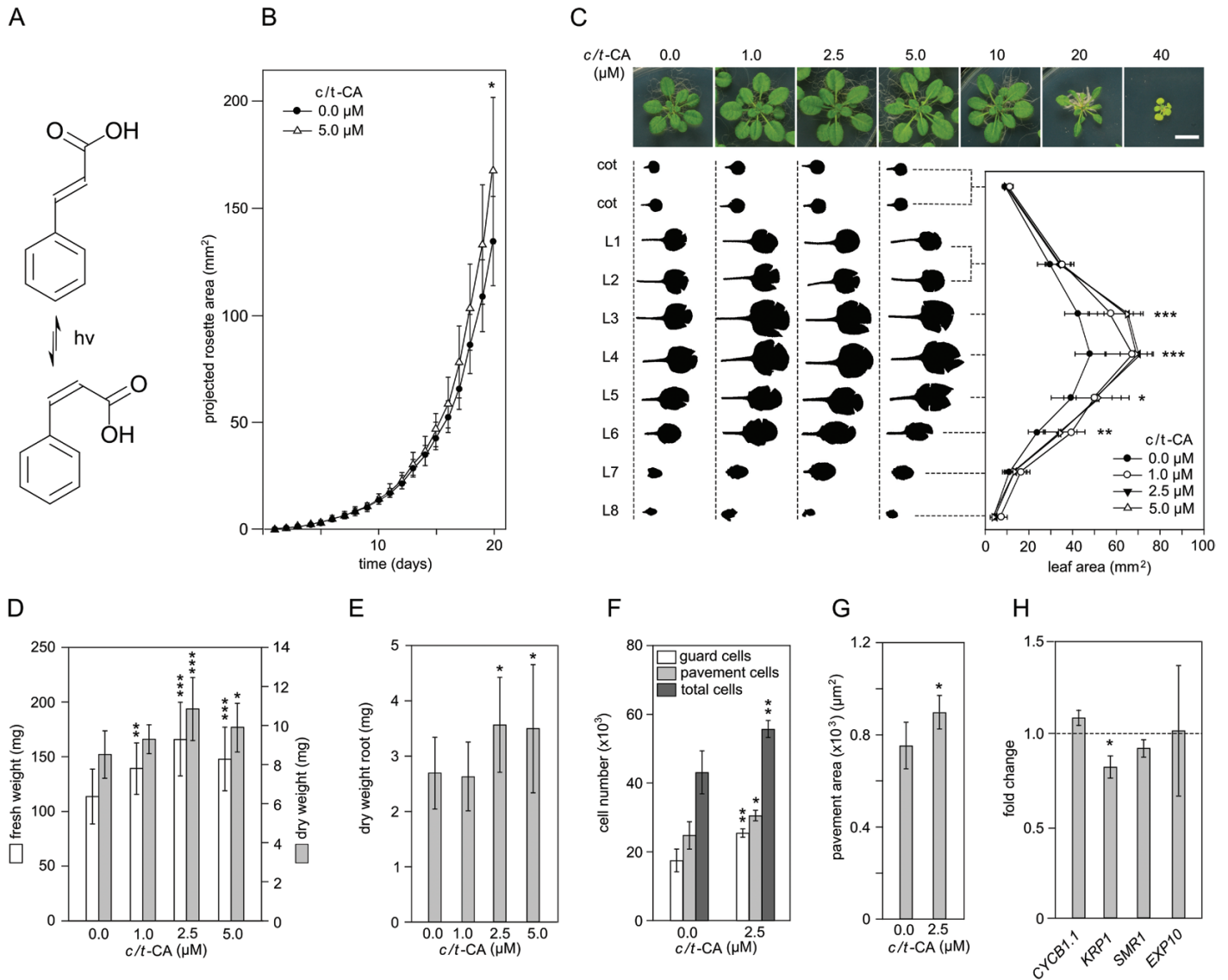


Fig. 1. Effect of *c/t*-CA on the growth of *A. thaliana*. (A) *c/t*-CA is an isomeric mixture of *t*-CA (top) and its photochemical conversion product *c*-CA (bottom). (B) Projected rosette area of *Arabidopsis* plants ($n > 18$ biological repeats) over time. Plants were grown on 0.5× MS medium with or without 5 μM *c/t*-CA and imaged on a 1 h interval basis over a period of 20 d starting from the moment stratification was stopped (DAS; days after stratification). For reasons of clarity, only a subset of the data points is shown (24 h interval). The average rosette area of plants grown at different *c/t*-CA concentrations are listed in Supplementary Table S2. (C) Rosette phenotype (top) and representative leaf series (bottom) of *Arabidopsis* plants at 20 DAS grown on 0.5× MS medium supplemented with different concentrations of *c/t*-CA (scale bar=0.5 cm). The area of individual leaves of plants ($n = 10$ biological repeats) was quantified and the average values were plotted. Labels on the y-axis correspond to the leaf (L) position. Because the two cotyledons as well as the first two developing leaves (L1–2) emerge simultaneously, no distinction was made between those leaves. The asterisks indicate significant differences between mock- and 5 μM *c/t*-CA-treated plants. Statistical differences for the other *c/t*-CA concentrations are given in Supplementary Table S3. (D) Rosette FW and DW of plants used in (B) at the end point of the growth experiment (20 DAS). The FW measurements were performed on individual plants ($n = 30$ biological repeats). For the DW measurements, pools of three plants were used to allow accurate quantification ($n = 10$). The values in the graph are averages on a single plant basis. (E) Root DW of plants used in (B) at 20 DAS. The measurements were performed on pools of 10 plants ($n > 12$ biological repeats), but the values in the graph are the averages on a single plant basis. (F) Number of guard cells, pavement cells, and total number of epidermal cells at the abaxial side of the third leaf ($n = 5$ biological repeats) of plants used in (C). (G) Area of pavement cells of the abaxial side at the base of the third leaf ($n = 5$ biological repeats) of plants used in (C). (H) Expression level of four growth-related genes in shoots of plants (10 DAS) growing on 0.5× MS medium supplemented with 2.5 μM *c/t*-CA compared with their expression in mock-treated plant ($n = 10$ biological repeats). Error bars represent the SD (except for H, where SEs were used) and asterisks indicate significant differences between *c/t*-CA-treated plants and the corresponding mock-treated plants as determined by Dunnett's test, except for (H), where significant differences were calculated using a two-sided Student's *t*-test. * $P < 0.05$, ** $P < 0.001$, *** $P < 0.0001$.

line with expectations, this increase in total leaf area was more pronounced as compared with the data obtained from the projected rosette areas. Because leaf series provide access to individual leaves, the most affected leaf could also be defined from this experiment. Although the fourth leaf was the largest at 20

DAS (68.5 mm²), the third leaf showed the highest increase in total area upon treatment with 2.5 μM *c/t*-CA when compared with the control (increase of 46% and 44% for the third and fourth leaf, respectively). Along with the leaf area data, a significant increase in rosette FW and DW was observed at the

final time point for the *c/t*-CA concentrations tested (Fig. 1D), with a maximal increase of 46% and 27% for FW and DW, respectively, at 2.5 μ M *c/t*-CA. The increase in biomass was not limited to the rosette, because roots of plants treated with 2.5 μ M and 5 μ M *c/t*-CA also had a higher DW compared with mock-treated plants at 20 DAS (an increase of 32% and 30%, respectively; Fig. 1E).

The observed increase in leaf area could result from the promotion of cell proliferation and/or cell expansion. To distinguish between both processes, cell drawings of the abaxial epidermis at the base of the third leaf were made for mock- and 2.5 μ M *c/t*-CA-treated plants. The third leaf was selected because it showed the highest increase in area upon treatment with 2.5 μ M *c/t*-CA compared with control plants. In addition, this leaf is fully expanded at the developmental stage at which the leaf series were made (20 DAS) (Gonzalez *et al.*, 2012). The cellular drawings were subsequently used to quantify the cell number and size of leaf epidermal cells using an automatic image analysis algorithm (Andriankaja *et al.*, 2012). This analysis revealed a significant increase in the number of guard and pavement cells in *c/t*-CA-treated plants compared with the control (an increase of 40% and 21%, respectively; Fig. 1F). Together with the cell number, the cell size of the pavement cells increased upon *c/t*-CA treatment (an increase of 19%) (Fig. 1G).

To find molecular support for the combined activity of cell proliferation and cell growth, the expression levels of marker genes for cell division [i.e. *KIP-RELATED POTEIN 1* (*KRP1*), *SIAMESE-RELATED 1* (*SMR1*), and *CYCLIN B1.1* (*CYCB1.1*)] and cell expansion [i.e. *EXPANSIN 10* (*EXP10*)] were quantified in shoots of seedlings at 10 DAS (Fig. 1H). The expression levels of *KRP1*, which is an inhibitor of cell division activity (Verkest *et al.*, 2005), decreased upon treatment with 2.5 μ M *c/t*-CA, corresponding to the observed increase in cell proliferation. The expression levels of the other genes

tested did not change, indicating that they are probably not (or no longer) involved in the *c/t*-CA-triggered leaf growth at the moment of sampling.

The growth-promoting activity of c/t-CA is not restricted to Arabidopsis

After the detailed growth analysis performed in Arabidopsis, the study was extended to *N. benthamiana*. Besides being a plant species belonging to a different family (*Brassicaceae* and *Solanaceae*, respectively), *N. benthamiana* has a different growth pattern. Whereas Arabidopsis forms a rosette during its vegetative stage and an inflorescence during its flowering stage, *N. benthamiana* does not go through a rosette and bolting stage, but immediately develops a stem. The more uniform growth pattern makes it a more suitable model for prolonged growth studies. To establish a working *c/t*-CA concentration for the growth assay, we initially determined the $IC_{50-root}$. *Nicotiana benthamiana* seeds were germinated on 0.5 \times Gamborg B5 medium supplemented with different concentrations of *c/t*-CA (1–10 μ M) and the primary root length was measured at 23 DAS (Supplementary Fig. S1A, B). Based on these data, the $IC_{50-root}$ value was calculated to be 3.5 μ M. In addition to inhibiting primary root growth, *c/t*-CA affected lateral roots, adventitious roots, and root hairs (Fig. 2A; Supplementary Fig. S1A–D). The growth-promoting activity of *c/t*-CA on the leaves of these relatively young plants was comparable with the effect described in Arabidopsis. A strong increase of the total leaf area was observed upon treatment with 1.0, 2.5, and 5.0 μ M *c/t*-CA (49, 41, and 17%, respectively) (Fig. 2B). Additionally, the FW of the entire shoot was increased by 63, 54, and 45%, respectively, for the different treatments, and the DW was higher in plants treated with 1 μ M and 2.5 μ M *c/t*-CA (an increase of 53% and 37%, respectively) (Fig. 2C).

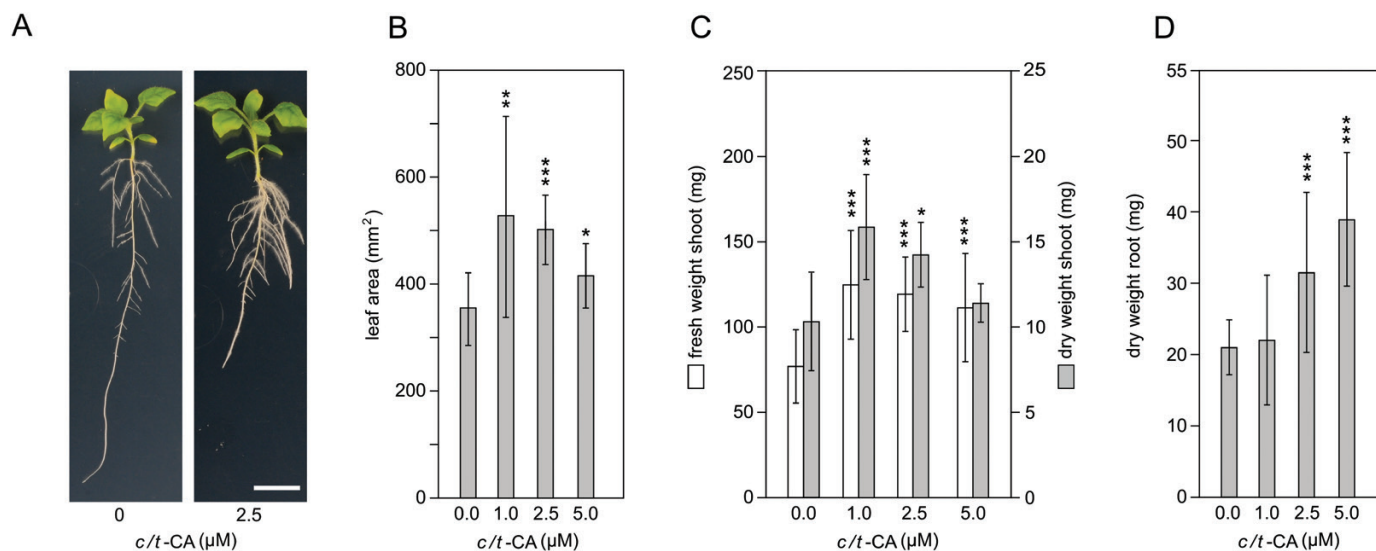


Fig. 2. Effect of *c/t*-CA on the growth of *N. benthamiana*. (A) *N. benthamiana* plants grown on 0.5 \times Gamborg B5 medium supplemented or not with *c/t*-CA at 14 DAS (scale bar=1 cm). (B) Total leaf area of plants (23 DAS; $n>11$ biological repeats) grown on 0.5 \times Gamborg B5 medium supplemented with different concentrations of *c/t*-CA. (C) Shoot FW and DW of plants grown as in (B). The FW measurements were performed on individual plants ($n>23$ biological repeats). For the DW measurements, pools of three plants were used ($n>6$ biological repeats), but the values in the graph are the averages on a single plant basis. (D) Root DW of plants ($n>27$ biological repeats) grown as in (B). Error bars represent SDs and asterisks indicate significant differences between *c/t*-CA-treated plants and the corresponding mock-treated plants as determined by Dunnett's test. * $P<0.05$, ** $P<0.001$, *** $P<0.0001$.

In parallel to the increase in above-ground biomass, the root biomass of 2.5 μM and 5 μM *c/t*-CA-treated plants increased compared with mock-treated plants (48% and 84%, respectively) (Fig. 2D).

To gain insight into the long-term effects of *c/t*-CA on plant growth, *N. benthamiana* seeds were germinated in plastic boxes on 0.5 \times Gamborg B5 medium in the presence of 2.5 μM *c/t*-CA. After 2 months, various growth parameters were determined. Compared with mock-treated controls, plants treated with *c/t*-CA were on average 19% taller and had stems that were on average 27% thicker (Fig. 3A–C). Together, this resulted in a 26% increase in FW of the above-ground plant biomass (Fig. 3D). When considering only the stem of the plants, the increase was 70% and 68% for the FW and DW, respectively (Fig. 3E). To evaluate whether the *c/t*-CA-mediated increase in stem diameter was accompanied by any anatomical perturbation, 60 μm thin transverse stem sections taken 1.0 cm above the root–stem junction of 2-month-old *in vitro* grown plants were investigated via bright-field microscopy. The sections revealed an overall expansion of the xylem in *c/t*-CA-treated plants. The expansion was the result of an increase of 32% in the number of xylem cells combined with an increase of 35% in the cross-sectional area of individual xylem cells (Fig. 3F, G). The average cell circularity (i.e. the ratio of the cell area to the perimeter) of the cell did not change upon *c/t*-CA treatment, indicating that the overall cross-sectional shape of the cell remained similar (Fig. 3H).

The role of auxin in *c/t*-CA-mediated biomass increase

Previous work on the mode of CA action revealed that auxin accumulates to high levels in *c/t*-CA treated roots, leading to a distinct root phenotype resembling auxin hypersensitivity (Steenackers *et al.*, 2017). To investigate the putative role of auxin in CA-mediated leaf growth, we re-examined the leaf growth-promoting effect of *c/t*-CA in *Arabidopsis* plants expressing *INDOLEACETIC ACID-LYSINE SYNTHETASE (iaaL)* of *Pseudomonas syringae* under the constitutive 35S promoter. The *iaaL* gene encodes an auxin-conjugating enzyme and consequently *p35S::iaaL* plants have artificially reduced indole-3-acetic acid (IAA) levels (Romano *et al.*, 1991). The rosettes of the *iaaL*-overexpressing line were much smaller compared with those of non-transformed control plants (Fig. 4A), underlining the importance of auxin for growth. When treated with 2.5 μM *c/t*-CA, wild-type plants produced more shoot biomass compared with the mock-treated plants (Fig. 4A, B), confirming previous results. This growth-promoting effect was absent in the *p35S::iaaL* plants (Fig. 4A, B; Supplementary Table S4), indicating that auxin (IAA) is indeed crucial for the leaf growth-promoting effect of *c/t*-CA.

To obtain further insight into potential shifts in auxin homeostasis in the leaves of *c/t*-CA-treated plants, the auxin-responsive marker *pDR5::GUS* line was grown on medium supplemented with 2.5 μM and 10 μM *c/t*-CA. As shown before (Steenackers *et al.*, 2017), a strong DR5-driven GUS activity was observed in primary root tips of *c/t*-CA-treated plants (Fig. 4C). Interestingly, the GUS pattern in the shoot was not different from that of mock-treated plants at 10 DAS,

suggesting that auxin is not accumulating in the rosette of plants growing on *c/t*-CA-containing medium (Fig. 4C). To confirm the root-specific auxin response, the expression levels of four genes involved in auxin homeostasis [*GRETCHEN HAGEN 3.2 (GH3.2)*, *GH3.3*, *GH3.5*, and *GH3.6*] were quantified in both root and shoot tissue of *Arabidopsis* seedlings (10 DAS) growing on medium to which 2.5 μM *c/t*-CA was added. In agreement with the DR5-driven GUS expression pattern in *c/t*-CA-treated seedlings, all *GH3* genes were exclusively up-regulated in the root tissue (Fig. 4D), indicating a CA-mediated accumulation of auxin in the root only. In parallel, we checked the expression levels of a shoot- and a root-specific auxin-induced gene [i.e. *SMALL AUXIN UP RNA19 (SAUR19)* and *LOB DOMAIN CONTAINING PROTEIN 16 (LBD16)*, respectively]. *LBD16* codes for a transcription activator of auxin-mediated lateral root initiation (Goh *et al.*, 2012) and, in line with the auxin-mediated induction of lateral root proliferation in CA-treated plants, the expression level of *LBD16* slightly increased in the roots of these plants (Fig. 4D). *SAUR19* links auxin to cell expansion in the leaves by blocking phosphatases that inactivate plasma membrane H^+ -ATPases (Spartz *et al.*, 2014). Although *SAUR19* expression is used as a readout for cell expansion (Spartz *et al.*, 2012), expression levels of this gene were not affected in the expanding leaves of CA-treated plants (Fig. 4D). The absence of change in gene expression could reflect a temporal condition; however, combined with the absence of a clear auxin response in the shoot, it implies that the CA-triggered growth increase is different from a canonical auxin-triggered induction of leaf growth. Evidence for independence between *c/t*-CA and the auxin-mediated leaf growth was found in the additive effect of *c/t*-CA on the increase in shoot biomass triggered by overexpression of *SAUR19* (Fig. 4E).

Together the data indicate that auxin, while being crucial for the growth-promoting effect of *c/t*-CA, is not directly involved at the level of the shoot to increase biomass. Accordingly, the effect on the shoot is likely to be the consequence of the auxin-dependent root proliferation in *c/t*-CA-treated plants.

Uncoupling the effect of *c*-CA and *t*-CA

The isomerization of CA is driven by UV-B (Clampitt and Callis, 1962), and the efficiency of the reaction depends on the duration of illumination and the intensity of the light source. We previously demonstrated that the amount of UV emitted by the tube lights (TLs) used in our plant growth rooms is sufficient to set a 60/40 *cis/trans*-CA equilibrium over the course of the experiment (Steenackers *et al.*, 2017). Consequently, the growth-promoting activity of *c/t*-CA could not be pinpointed to one of the isomers under the given settings. To exclude photo-isomerization of CA during plant growth, plants were grown as described above on 0.5 \times MS medium supplemented with pure *c*- or *t*-CA under light-emitting diode (LED) lighting in contrast to TLs. The spectra of both light sources are different, but the important point for this experiment was the absence of UV-B in the LED spectrum as opposed to that of TL (Fig. 5A, B). Under these conditions, *c*-CA altered the root architecture of *Arabidopsis* plants (i.e. an increase in number of

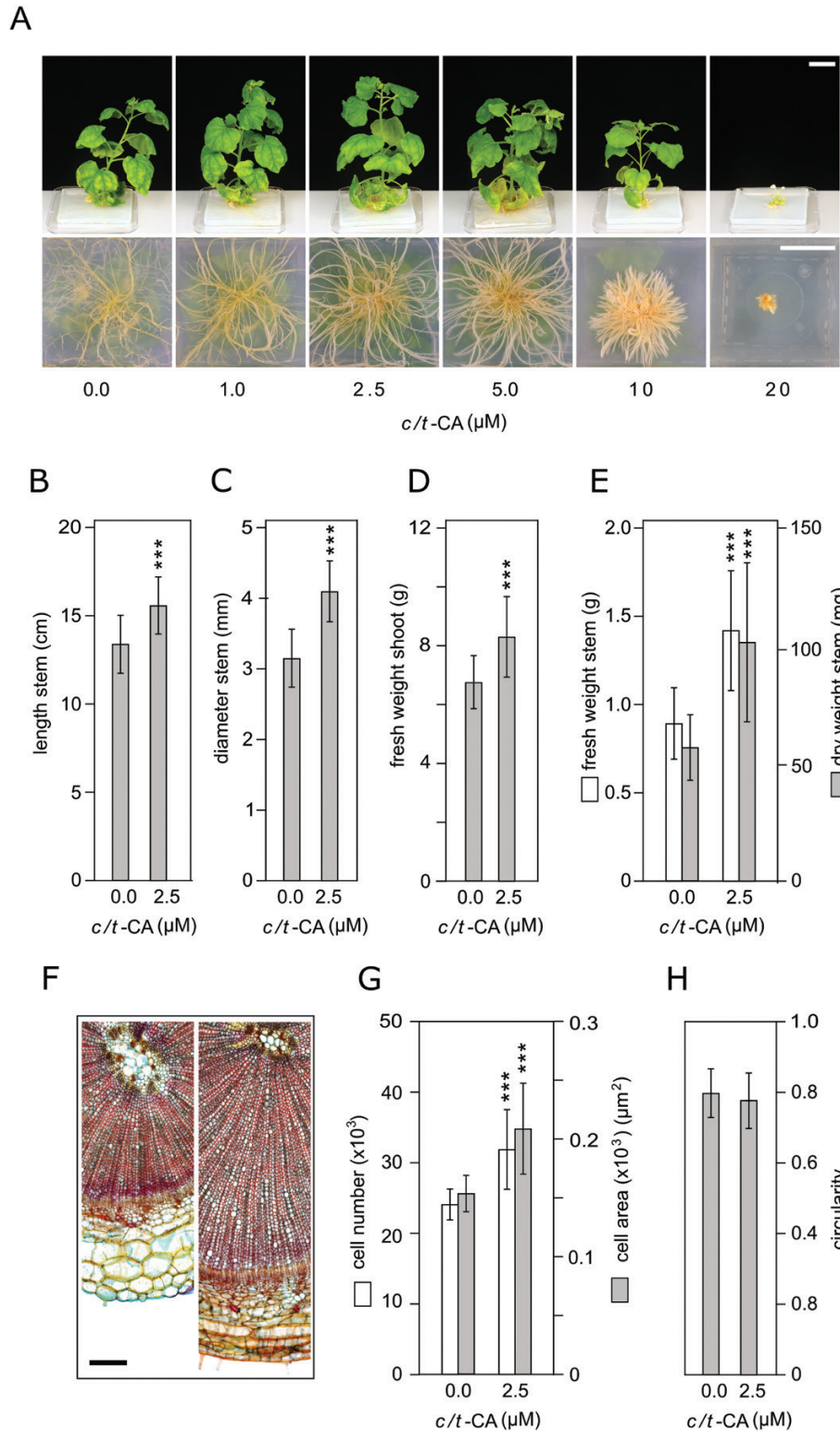


Fig. 3. Effect of long-term treatment with *c/t*-CA on the growth of *N. benthamiana*. (A) Two-month-old *N. benthamiana* plants grown on 0.5× Gamborg B5 medium supplemented with different concentrations of *c/t*-CA (scale bar=4.0 cm). Top: front view of the shoot. Bottom: bottom view of the root system. (B) Stem length of 2-month-old *N. benthamiana* plants ($n=20$ biological repeats) grown on 0.5×Gamborg B5 medium supplemented or not with 2.5 μM *c/t*-CA. (C) Diameter of the stem measured 1 cm above the root–shoot junction of the plants ($n=20$ biological repeats) used in (B). (D) Shoot FW of the plants used in (B). (E) Stem FW and DW of the plants grown as in (B). (F) Representative cross-sections from the base of the stem 1 cm above the root–shoot junction of 2-month-old plants grown on 0.5× Gamborg B5 medium supplemented (right) or not (left) with 2.5 μM *c/t*-CA. Sections were made with a vibratome, triple stained (i.e. astra blue, chrysoidine, and acridine red), and imaged under a bright-field microscope (scale bar=250 μm). (G) Number and area of xylem cells in stem cross-sections ($n=3$ biological repeats) of the plants as used in (F). (H) Circularity of xylem cells of cross-sections ($n=3$ biological repeats) as used in (F). Circularity is defined as $4\pi A/P^2$, in which A and P equal the cell area and perimeter, respectively. Error bars represent SDs and asterisks indicate significant differences between *c/t*-CA-treated plants and the corresponding mock-treated plants as determined by Dunnett’s test. * $P<0.05$, ** $P<0.001$, *** $P<0.0001$.

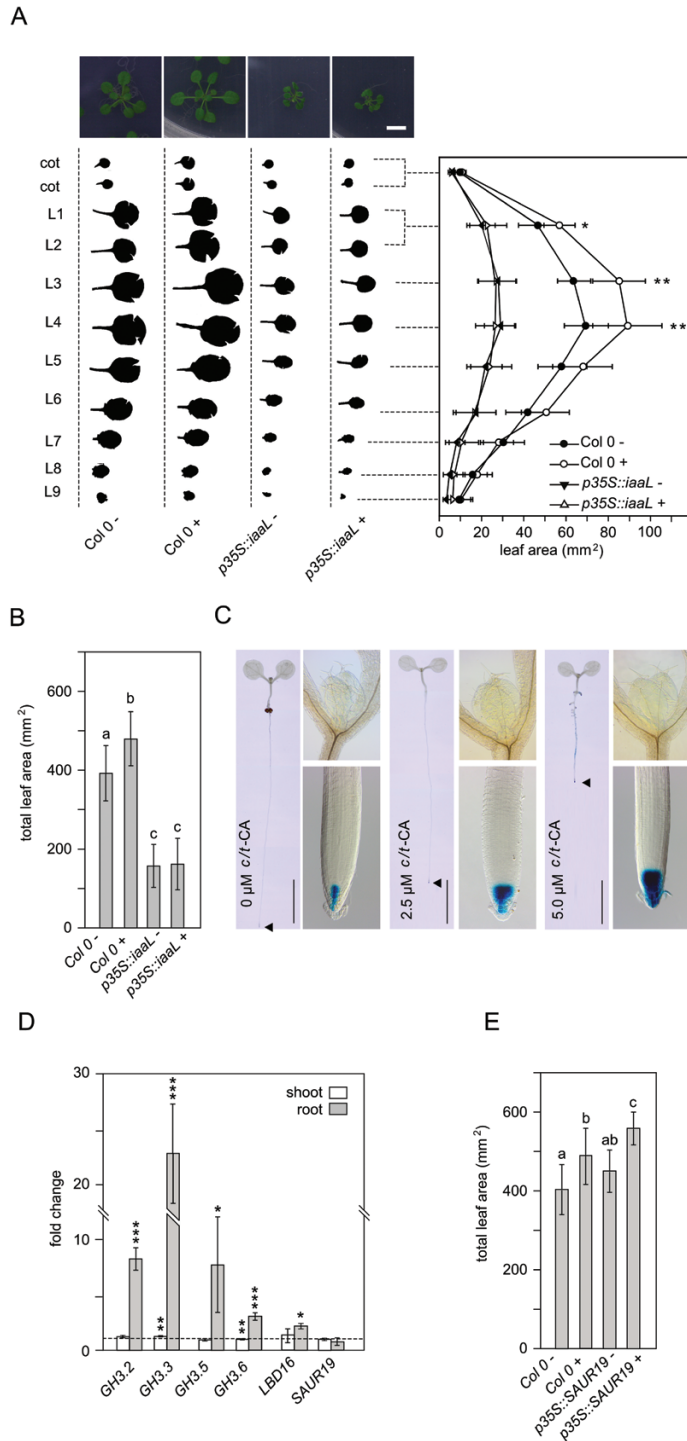


Fig. 4. Essential role of auxin in the growth-promoting activity of *c*-CA. (A) Rosette phenotype (top) and representative leaf series (bottom) of WT (Col-0) and *p35S::iaaL* Arabidopsis plants grown on 0.5× MS medium supplemented (+) or not (–) with 2.5 μM *c/t*-CA at 20 DAS (scale bar=1 cm). The area of individual leaves of plants ($n > 10$ biological repeats) was quantified and the average values were plotted in a graph. Labels on the y-axis correspond to the leaf (L) position. Because the two cotyledons as well as the first two developing leaves (L1–2) emerge simultaneously, no distinction was made between those leaves. (B) Total leaf area of the plants ($n > 10$ biological repeats) used in (A). (C) DR5-driven *GUS* expression in Arabidopsis plants grown on 0.5× MS medium supplemented with different concentrations of *c/t*-CA at 7 DAS. Arrowheads point to the position of the primary root tip (scale bars=1 cm). (D) Relative expression level of auxin-related genes in shoot and root of

adventitious roots, lateral roots, and root hair density), whereas plants grown on a similar concentration of *t*-CA were indistinguishable from mock-treated plants (Fig. 5C; Supplementary Fig. S2A–D). A concentration of 1 μM *c*-CA had a stimulatory effect on plant biomass (FW increase of 46%), whereas a higher concentration of *c*-CA (2.5 μM) did not (Fig. 5D), indicating that a supra-optimal concentration was reached. Plants treated with different *t*-CA concentrations did not show any significant increase in FW in comparison with mock-treated control plants (Fig. 5D).

Although the results support the hypothesis that the growth-promoting activity of CA is restricted to its *cis*-isomer, a drawback remains that plants were grown under different environmental conditions (i.e. lights with a different spectrum; Fig. 5A, B). To provide complementary evidence on the growth-promoting activity of *c*-CA, photo-isomerization of CA was prevented by changing the compound as opposed to changing the light conditions. CA was replaced by *trans*- or *cis*-PCPCA, which are considered to be structurally stabilized analogs of *t*- and *c*-CA, respectively (Veldstra and Van De Westeringh, 1951; Abe *et al.*, 2012). In fact, PCPCA occurs in four distinct stereoisomers because it has two chiral carbon atoms. The two stereoisomers of what is considered *t*-PCPCA [i.e. (1*S*,2*S*)-PCPCA and (1*R*,2*R*)-PCPCA] have their substituents on opposite sides of the plane formed by the cyclopropane ring, whereas for *c*-PCPCA [i.e. (1*S*,2*R*)-PCPCA and (1*R*,2*S*)-PCPCA] both substituents are on the same side (Fig. 6A).

While setting the optimal compound concentration range of *c*- and *t*-PCPCA for the growth analyses, it became clear that Arabidopsis grown on 0.5× MS medium supplemented with different concentrations of *c*-PCPCA (0.25–5 μM) phenocopied *c*-CA-treated plants. This was in contrast to *t*-PCPCA, which had no effect on plant growth when used at equimolar concentrations (Fig. 6B; Supplementary Fig. S3) analogous to *t*-CA. The *c*-PCPCA concentration needed to reduce the primary root length by 50% ($IC_{50-root}$) was determined to be 2.0 μM. Based on this value, a concentration range was established (i.e. 0.25, 0.5, and 1 μM) and a detailed time-lapse growth analysis was performed as described above (Fig. 6C; Supplementary Table S5). At 13 DAS, the projected rosette area of plants treated with 0.25 μM *c*-PCPCA began to deviate from that of mock-treated plants (an increase of 10%). This difference further increased over time, resulting in a final significant increase in the projected rosette area of 25% at the end of the experiment (i.e. 20 DAS). When *c*-PCPCA was applied at a slightly higher concentration (0.5 μM), the growth-promoting

Arabidopsis plants (10 DAS) grown on 0.5× MS medium supplemented with 2.5 μM *c/t*-CA. The expression levels of the genes are shown as fold change compared with the expression level in mock-treated Arabidopsis plants ($n = 10$ biological repeats). (E) Total leaf area of WT and *p35S::GFP-SAUR19* Arabidopsis plants at 20 DAS, grown on 0.5× MS medium supplemented (+) or not (–) with 2.5 μM *c/t*-CA. Error bars represent SDs and asterisks indicate significant differences between *c/t*-CA-treated plants and the corresponding mock-treated plants as determined by Dunnett's test (* $P < 0.05$, ** $P < 0.001$, *** $P < 0.0001$), except for (D), where significant differences were calculated using a two-sided Student's *t*-test and where different letters indicate significant difference ($P \leq 0.05$) between means.

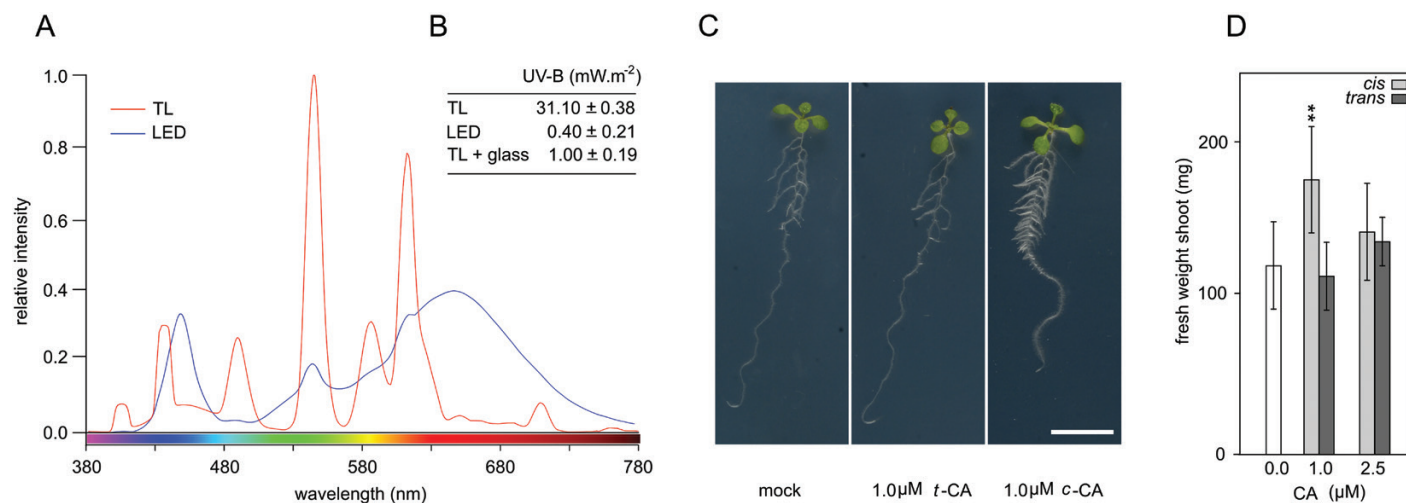


Fig. 5. *A. thaliana* grown under LED lights to avoid isomerization of CA. (A) Spectral power distribution of the fluorescent tube lights (TLs) and LED lights of the growth cabinets used in this study to grow *Arabidopsis* plants. (B) Amount of UV-B emitted by the TL and LED lights of the growth cabinets for which the spectral power distribution is shown in (A). Because glass blocks UV-B radiation, 'TL+glass' (glass-shielded TL source) was added as a control to set a baseline. (C) Phenotype of plants grown on 0.5× MS medium (left) or in the presence of *t*- (middle) or *c*-CA (right) (scale bars=1 cm). (D) Rosette FW of *Arabidopsis* plants ($n > 28$ biological repeats) at 20 DAS. Plants were grown on 0.5× MS medium supplemented with *c*- or *t*-CA. The plants were grown under LED conditions to avoid UV-B-mediated isomerization of *c*- and *t*-CA.

effect was delayed, and the treated plants showed only a 13% increase in projected rosette area at the final time point. It is noteworthy that the highest concentration tested (1 μM) had no positive effect on the projected rosette area. Hence, the growth effects follow a dose–response curve typical for bioactive molecules, whereby toxic effects are obtained when supra-optimal concentrations are applied. At the end of the experiment, individual leaf areas were calculated via leaf series as described above (Fig. 6D; Supplementary Table S6). For both the projected and actual leaf area, 0.25 μM *c*-PCPCA gave the highest increase compared with mock-treated plants (an increase of 25% and 33%, respectively).

Together, these data underline that the *cis*-isomer and not the *trans*-isomer of CA is causal of the growth-promoting effect in *c/t*-CA treated plants.

Discussion

c-CA is a natural compound of plant origin that triggers lateral and adventitious root proliferation when exogenously supplied to seedlings (Wong *et al.*, 2005; Steenackers *et al.*, 2017). The resulting development of an elaborate root system could be beneficial to plants, because it allows exploration of a larger area for resources (Werner *et al.*, 2001), which could result in an increased shoot growth. In line with this hypothesis, we found with *c/t*-CA a 32% and 49% increase in leaf area in *Arabidopsis* and *N. benthamiana*, respectively. Despite the use of an isomeric mixture of CA, we only considered the bioactive *cis*-isomer to be responsible for the growth-promoting activity. To find supporting evidence for our hypothesis, we tested photochemically stable structural analogs of *c*- and *t*-CA for their growth-promoting activity. In parallel we also tested the growth-promoting activity of pure *c*- and *t*-CA under light conditions lacking UV, to avoid the isomerization of CA

during the course of the experiment. In both cases, the *cis*-form acted as a YPC, whereas the *trans*-form was inactive. Most probably the previously claimed activity of *t*-CA (Talaat and Balbaa, 2010; Singh *et al.*, 2013; Kurepa *et al.*, 2018) was the result of unintended isomerization of *t*-CA towards the bioactive *c*-CA during the course of the experiment, a recurring problem in studies on bioactive phenylpropanoids (Vanholme *et al.*, 2019).

The identification of *c*-CA as a growth-promoting compound paves the way to obtain novel, more efficient, or even species-specific agrochemicals. Here we can rely on structure–activity relationship (SAR) studies that have been performed on a *c*-CA scaffold, using the inhibition of primary root growth as readout for the compounds' activity (Abe *et al.*, 2012; Nishikawa *et al.*, 2013a, b). Although the goal of these studies was to find novel herbicides, the reported hit compounds could also have growth-promoting effects when used at lower doses. In line with the difference in activity observed between the *cis*- and *trans*-isomers, the SAR studies revealed the importance of the spatial orientation of the carboxyl side chain for the activity. Also the stabilization of the side chain with higher order ring structures as well as small modifications to the phenyl moiety were reported as modifications that increase efficacy (Abe *et al.*, 2012; Nishikawa *et al.*, 2013a, b). One of these structural analogs was tested here and showed growth improvement at concentrations 10× lower than the *t/c*-CA mixture, further underlining the valorization potential of CA as lead compound for novel YPCs.

The molecular model underlying the leaf growth-promoting property of CA remains enigmatic and, although auxin seems to have a crucial role, auxin-independent mechanisms cannot be excluded (Kurepa and Smalle, 2019). The model we present is based on the *c*-CA-mediated inhibition of IAA transport in the primary root tip, which lies at the basis of the observed auxin response in the roots of plants grown on *c*-CA-containing

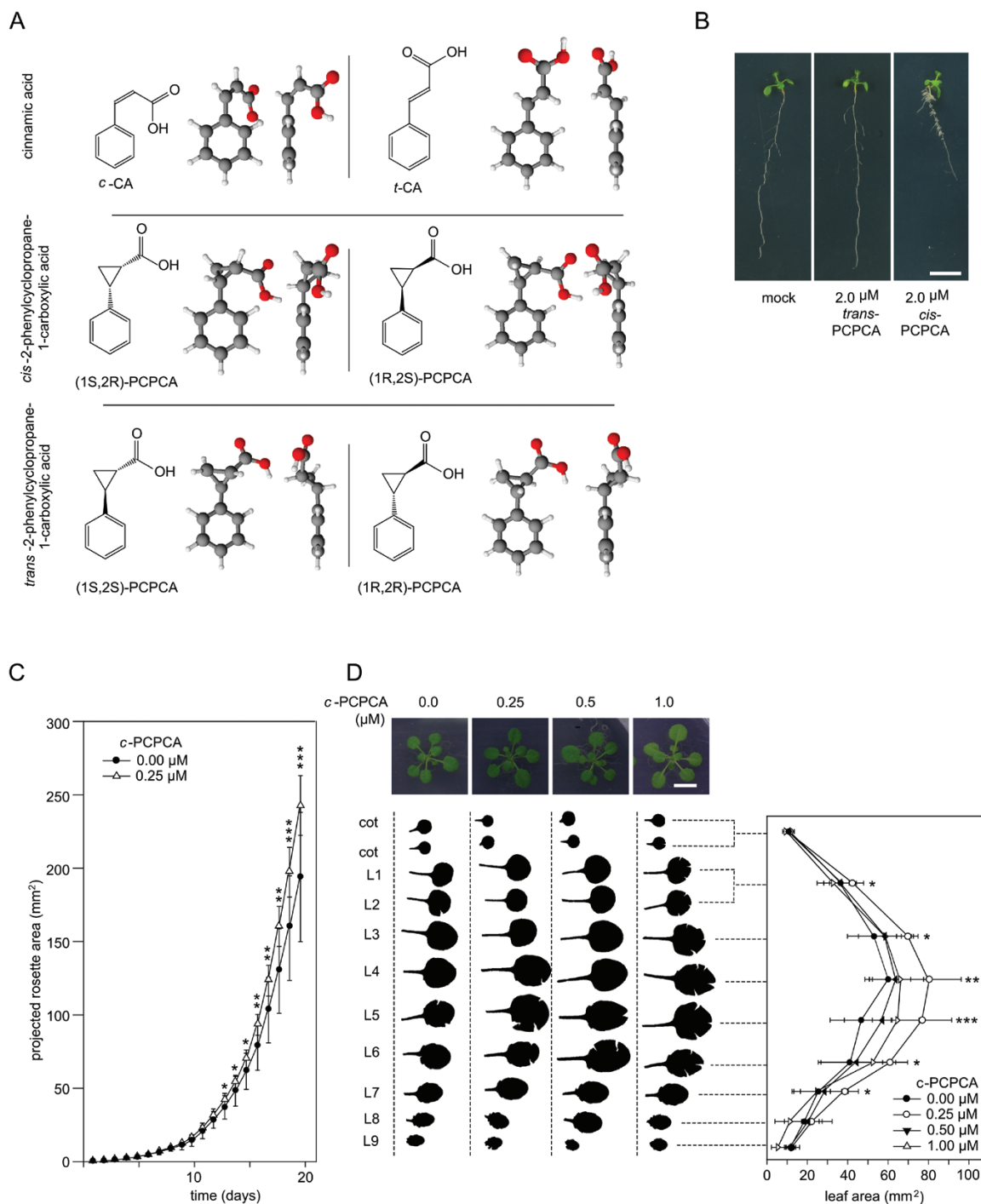


Fig. 6. Effect of 2-phenylcyclopropane-1-carboxylic acid (PCPCA) on the growth of *A. thaliana*. (A) Structure of two CA isomers (*trans/cis*) and four PCPCA stereoisomers (1S,2R/1R,2S/1S,2S/1R,2R). For each of the compounds, the 2D skeletal formula is accompanied by a 3D projection depicted as the front and side view. No light-mediated conversion between the different PCPCA isomers is possible. (B) Arabidopsis plants at 10 DAS grown on 0.5 \times MS medium supplemented with 2 μM *t*- or *c*-PCPCA (scale bar=1 cm). (C) Projected rosette area of Arabidopsis plants ($n=12$ biological repeats) over time. Plants were grown on 0.5 \times MS medium with or without 0.25 μM *c*-PCPCA and imaged every hour for 20 d. For clarity, only a subset of the data points is shown (24 h interval). The average rosette area of plants grown at different concentrations of *c/t*-PCPCA are listed in Supplementary Table S5. (D) Rosette phenotype (top) and representative leaf series (bottom) of Arabidopsis plants ($n=10$ biological repeats) at 20 DAS, grown on 0.5 \times MS medium supplemented with different concentrations of *c*-PCPCA (scale bar=0.5 cm). The area of individual leaves of plants ($n>11$ biological repeats) was quantified and the average values were plotted. Labels on the *y*-axis correspond to the leaf (L) position. Because the two cotyledons as well as the first two developing leaves (L1–2) emerge simultaneously, no distinction was made between those leaves. The asterisks indicate significant differences between mock- and 0.25 μM *c*-PCPCA-treated plants. Statistical differences for the other *c*-PCPCA concentrations are given in Supplementary Table S6. Error bars represent SDs and asterisks indicate significant differences between *c/t*-PCPCA-treated plants and the corresponding mock-treated plants as determined by Dunnett's test. * $P<0.05$, ** $P<0.001$, *** $P<0.0001$.

medium (Vanholme *et al.*, 2019). An interesting point is that a similar response is not detected in the above-ground tissue (Wasano *et al.*, 2013). Although this could indicate that the *c*-CA target is not present in the shoot at that developmental stage, an alternative explanation could be that *c*-CA is not translocated from the root to the shoot. In support of the latter, there are some old studies reporting on the immobility of *c*-CA in plant tissue (Haagen Smit and Went, 1935; Went and White, 1939). In contrast to *c*-CA, IAA is known to be mobile in plants, and the potential difference in mobility between both compounds could explain the unique growth-promoting property of *c*-CA. The immobile *c*-CA acts locally in the root tissue where it affects the root architecture by trapping IAA. Exogenously supplied auxin, on the other hand, quickly finds its way to the shoot, where it will disturb tightly regulated local auxin gradients crucial for proper growth and development. In seeming contradiction to this model are the reports on the positive effect of exogenously supplied IAA on shoot biomass (Contreras-Cornejo *et al.*, 2009). However, these effects are only observed when auxin is used at very low concentrations (<60 nM). Because plant roots are more sensitive to auxin compared with the shoot, low auxin concentrations will alter the root architecture without negatively impacting the shoot. Hence, here also the increase in shoot biomass could be the consequence of the increased water and nutrient uptake efficiency of the roots, bringing these observations in line with our suggested model.

Another strong support for our hypothesis is the ‘auxin after effect’ (Thimann and Lane, 1938) or ‘hormonization’ (Cholodny, 1936), describing the accelerated growth of plants following a temporary treatment with high auxin concentrations (up to 0.5 mM). According to Thimann (1938), the supplied auxin triggers massive root formation at the expense of plant growth. Once released from the auxin, the initiated root primordia quickly develop into lateral roots, resulting in plants with an elaborated root system, giving the treated plants an advantage, enabling them to quickly catch up with the controls and even outperform them. This effect can to some extent be phenocopied by the root-specific expression of a gene encoding a cytokinin-degrading CYTOKININ OXIDASE/DEHYDROGENASE (CKX). The consequently reduced cytokinin levels in the root tips alter the auxin–cytokinin balance in favor of auxin. As a result, these plants have a more elaborate root system without negatively impacting the shoot. In addition to an improved nutrient uptake, *P10::CKX3* transgenic Arabidopsis plants had a 17% increase in rosette diameter and a 37% increase in FW (Werner *et al.*, 2010).

In conclusion, our data bring *c*-CA front and center as an appealing lead compound representing a novel class of growth-promoting agrochemicals. CA is a simple natural molecule, one enzymatic step away from the aromatic amino acid phenylalanine, and is easy to synthesize from elementary chemical building blocks. In addition, UV-B light is all that is needed to convert the cheap but inactive *t*-CA to its bioactive *cis*-isoform, providing opportunities to implement it in innovative and sustainable plant growth systems that are currently used in vertical and urban farming.

Supplementary data

Supplementary data are available at *JXB* online

Fig. S1. Effect of *c/t*-CA on *N. benthamiana* root growth and development.

Fig. S2. Effect of *c*-CA and *t*-CA on *A. thaliana* grown under LED conditions.

Fig. S3. Effect of *c*- and *t*-PCPCA on *A. thaliana* root growth and development.

Table S1. List of primers used in this research.

Table S2. Growth-promoting effect of *c/t*-CA on *A. thaliana*.

Table S3. Growth-promoting effect of *c/t*-CA on *A. thaliana* leaves.

Table S4. Growth-promoting effect of *c*-CA on *A. thaliana* *p35S::iaaL* and wild-type (Col-0) leaves.

Table S5. Growth-promoting effect of *c*-PCPCA on *A. thaliana*.

Table S6. Growth-promoting effect of *c*-PCPCA on *A. thaliana* leaves.

Acknowledgements

The work on bioactive phenylpropanoids is supported by the Research Foundation Flanders under project numbers G008116N and 1S04018N, and a post-doctoral fellowship to SD. The plant phenotyping platforms are supported by Ghent University (‘Bijzonder Onderzoeksfonds Methusalem project’ no. BOF08/01M00408). The authors would like to thank Wouter Claes for substantial technical assistance in performing the experiments, Karel Spruyt for assistance in imaging, Stefaan Werbrouck for LED plant growth facilities, and Ottoline Leyser (Sainsbury Laboratory, University of Cambridge) for providing *p35S::iaaL* Arabidopsis seeds.

References

- Abe M, Nishikawa K, Fukuda H, *et al.* 2012. Key structural features of *cis*-cinnamic acid as an allelochemical. *Phytochemistry* **84**, 56–67.
- Andriankaja M, Dhondt S, De Bodt S, *et al.* 2012. Exit from proliferation during leaf development in *Arabidopsis thaliana*: a not-so-gradual process. *Developmental Cell* **22**, 64–78.
- Arnao MB, Hernández-Ruiz J. 2019. Melatonin: a new plant hormone and/or a plant master regulator? *Trends in Plant Science* **24**, 38–48.
- Baekelandt A, Pauwels L, Wang Z, *et al.* 2018. Arabidopsis leaf flatness is regulated by PPD2 and NINJA through repression of CYCLIN D3 genes. *Plant Physiology* **178**, 217–232.
- Beeckman T, Engler G. 1994. An easy technique for the clearing of histochemically stained plant tissue. *Plant Molecular Biology Reporter* **12**, 37–42.
- Chavas JP, Mitchell PD. 2018. Corn productivity: the role of management and biotechnology. In: Amanullah, Fahad S, eds. *Corn—production and human health in changing climate*. InTech, doi: 10.5772/intechopen.77054.
- Cholodny NG. 1936. Hormonization of grains. *Comptes Rendus (Doklady) de l’Académie des Sciences de l’URSS* **3**, 439–442.
- Clampitt BH, Callis JW. 1962. Photochemical isomerization of cinnamic acid in aqueous solutions. *Journal of Physical Chemistry* **66**, 201–204.
- Contreras-Cornejo HA, Macías-Rodríguez L, Cortés-Penagos C, López-Bucio J. 2009. *Trichoderma virens*, a plant beneficial fungus, enhances biomass production and promotes lateral root growth through an auxin-dependent mechanism in Arabidopsis. *Plant Physiology* **149**, 1579–1592.
- Depuydt S, Hardtke CS. 2011. Hormone signalling crosstalk in plant growth regulation. *Current Biology* **21**, R365–R373.
- Dhondt S, Gonzalez N, Blomme J, De Milde L, Van Daele T, Van Akoleyen D, Storme V, Coppens F, Beemster GTS, Inzé D. 2014.

High-resolution time-resolved imaging of in vitro Arabidopsis rosette growth. *The Plant Journal* **80**, 172–184.

Evenson RE, Gollin D. 2003. Assessing the impact of the green revolution, 1960 to 2000. *Science* **300**, 758–762.

Goh T, Joi S, Mimura T, Fukaki H. 2012. The establishment of asymmetry in Arabidopsis lateral root founder cells is regulated by LBD16/ASL18 and related LBD/ASL proteins. *Development* **139**, 883–893.

Gonzalez N, Vanhaeren H, Inzé D. 2012. Leaf size control: complex coordination of cell division and expansion. *Trends in Plant Science* **17**, 332–340.

Haagen Smit AJ, Went FW. 1935. A physiological analysis of the growth substance. *Proceedings of the Royal Academy of Sciences at Amsterdam* **38**, 852–857.

Hake S, Ross-Ibarra J. 2015. Genetic, evolutionary and plant breeding insights from the domestication of maize. *eLife* **4**, e05861.

Hardeland R. 2016. Melatonin in plants—diversity of levels and multiplicity of functions. *Frontiers in Plant Science* **7**, 198.

Hufford MB, Xu X, van Heerwaarden J, et al. 2012. Comparative population genomics of maize domestication and improvement. *Nature Genetics* **44**, 808–811.

Kick H. 1953. Pflanzenertrag und Nährstoffaufnahme bei Düngung mit wuchsstoffartigen Stoffen. *Zeitschrift für Pflanzenernährung, Düngung, Bodenkunde* **63**, 30–37.

Kruyt W. 1954. A study in connection with the problem of hormonization of seeds. *Acta Botanica Neerlandica* **3**, 1–82.

Kurepa J, Shull TE, Karunadasa SS, Smalle JA. 2018. Modulation of auxin and cytokinin responses by early steps of the phenylpropanoid pathway. *BMC Plant Biology* **18**, 278.

Kurepa J, Smalle JA. 2019. *trans*-Cinnamic acid-induced leaf expansion involves an auxin-independent component. *Communicative & Integrative Biology* **12**, 78–81.

Leopold AC. 1955. Auxin and plant growth. Berkeley: University of California Press.

Liu Z, Garcia A, McMullen MD, Flint-Garcia SA. 2016. Genetic analysis of kernel traits in maize–teosinte introgression populations. *G3* **6**, 2523–2530.

Nishikawa K, Fukuda H, Abe M, et al. 2013a. Substituent effects of *cis*-cinnamic acid analogues as plant growth inhibitors. *Phytochemistry* **96**, 132–147.

Nishikawa K, Fukuda H, Abe M, Nakanishi K, Tazawa Y, Yamaguchi C, Hiradate S, Fujii Y, Okuda K, Shindo M. 2013b. Design and synthesis of conformationally constrained analogues of *cis*-cinnamic acid and evaluation of their plant growth inhibitory activity. *Phytochemistry* **96**, 223–234.

Romano CP, Hein MB, Klee HJ. 1991. Inactivation of auxin in tobacco transformed with the indoleacetic acid-lysine synthetase gene of *Pseudomonas savastanoi*. *Genes & Development* **5**, 438–446.

Schneider CA, Rasband WS, Eliceiri KW. 2012. NIH Image to ImageJ: 25 years of image analysis. *Nature Methods* **9**, 671–675.

Singh PK, Singh R, Singh S. 2013. Cinnamic acid induced changes in reactive oxygen species scavenging enzymes and protein profile in maize (*Zea mays* L.) plants grown under salt stress. *Physiology and Molecular Biology of Plants* **19**, 53–59.

Spartz AK, Lee SH, Wenger JP, Gonzalez N, Itoh H, Inzé D, Peer WA, Murphy AS, Overvoorde PJ, Gray WM. 2012. The SAUR19 subfamily of SMALL AUXIN UP RNA genes promote cell expansion. *The Plant Journal* **70**, 978–990.

Spartz AK, Ren H, Park MY, Grandt KN, Lee SH, Murphy AS, Sussman MR, Overvoorde PJ, Gray WM. 2014. SAUR inhibition of PP2C-D phosphatases activates plasma membrane H₊-ATPases to promote cell expansion in Arabidopsis. *The Plant Cell* **26**, 2129–2142.

Steenackers W, Klíma P, Quareshy M, et al. 2017. *cis*-Cinnamic acid is a novel, natural auxin efflux inhibitor that promotes lateral root formation. *Plant Physiology* **173**, 552–565.

Talaat IM, Balbaa LK. 2010. Physiological response of sweet basil plants (*Ocimum basilicum* L.) to putrescine and *trans*-cinnamic acid. *American-Eurasian Journal of Agricultural & Environmental Sciences* **8**, 438–445.

Thimann KV, Lane RN. 1938. After-effects of the treatment of seed with auxin. *American Journal of Botany* **25**, 535–543.

Van Dingenen J, Antoniou C, Filippou P, Pollier J, Gonzalez N, Dhondt S, Goossens A, Fotopoulos V, Inzé D. 2017. Strobilurins as growth-promoting compounds: how Strobly regulates Arabidopsis leaf growth. *Plant, Cell & Environment* **40**, 1748–1760.

Vanhaeren H, Inzé D, Gonzalez N. 2016. Plant growth beyond limits. *Trends in Plant Science* **21**, 102–109.

Vanholme B, El Houari I, Boerjan W. 2019. Bioactivity: phenylpropanoids' best kept secret. *Current Opinion in Biotechnology* **56**, 156–162.

Veldstra H, Van De Westeringh C. 1951. 2-Phenyl-cyclopropan-1-carboxylic acids. *Recueil Des Travaux Chimiques Des Pays-Bas* **70**, 1127–1135.

Verkest A, Weini C, Inzé D, De Veylder L, Schnittger A. 2005. Switching the cell cycle. KIP-related proteins in plant cell cycle control. *Plant Physiology* **139**, 1099–1106.

Wasano N, Sugano M, Nishikawa K, et al. 2013. Root-specific induction of early auxin-responsive genes in *Arabidopsis thaliana* by *cis*-cinnamic acid. *Plant Biotechnology* **30**, 465–471.

Went FW, White R. 1939. Experiments on the transport of auxin. *Botanical Gazette* **100**, 465–484.

Werner T, Motyka V, Strnad M, Schömlling T. 2001. Regulation of plant growth by cytokinin. *Proceedings of the National Academy of Sciences, USA* **98**, 10487–10492.

Werner T, Nehnevajova E, Köllmer I, Novák O, Strnad M, Krämer U, Schömlling T. 2010. Root-specific reduction of cytokinin causes enhanced root growth, drought tolerance, and leaf mineral enrichment in Arabidopsis and tobacco. *The Plant Cell* **22**, 3905–3920.

Willard W. 1938. Some experiments with auxin A and other growth factors. Master thesis, Departement of Botany, University of British Columbia.

Wong WS, Guo D, Wang XL, Yin ZQ, Xia B, Li N. 2005. Study of *cis*-cinnamic acid in *Arabidopsis thaliana*. *Plant Physiology and Biochemistry* **43**, 929–937.

Yakhin OI, Lubyantsov AA, Yakhin IA, Brown PH. 2016. Biostimulants in plant science: a global perspective. *Frontiers in Plant Science* **7**, 2049.

Yin Z, Wong W, Ye W, Li N. 2003. Biologically active *cis*-cinnamic acid occurs naturally in *Brassica parachinensis*. *Chinese Science Bulletin* **48**, 555–558.